Journal of
Materials Chemistry B

Accepted Manuscript

This article can be cited before page numbers have been issued, to do this please use: M. Zou, D. Li, R. Yuan and Y. Xiang, *J. Mater. Chem. B*, 2018, DOI: 10.1039/C8TB00610E.

ROYAL SOCIETY OF CHEMISTRY

rsc.li/materials-b

View Article Online
DOI: 10.1039/C8TB00610E

Journal Name

ARTICLE

A target-responsive autonomous aptamer machine biosensor for enzyme-free and sensitive detection of protein biomarkers

Received 00th January 20xx,
Accepted 00th January 20xx

DOI: 10.1039/x0xx00000x

www.rsc.org/

Mengqi Zou,[a] Daxiu Li,[a] Ruo Yuan,[a] Yun Xiang*[a]

Highly sensitive and selective detection of protein disease markers is crucial for fundamental research and disease diagnosis. In this work, based on a new target-triggered autonomous aptamer machinery amplification approach, we developed a simple and sensitive sensing platform for the detection of a cancer biomarker, platelet-derived growth factor BB (PDGF-BB), in human serums. The target PDGF-BB binds the fluorescently quenched hairpin aptamer probes and causes the structure conformational change of the aptamers to recover the fluorescence. The presence of the partial duplex DNA fuel strands further leads to the recycling of the target proteins and the function of the aptamer machine autonomously to amplify the fluorescence emission significantly, thereby resulting in sensitive detection of PDGF-BB down to the low picomolar level. Besides, due to the high specificity of the aptamer, such a protein detection method shows high selectivity and can be employed to detect PDGF-BB in human serums. Featuring with the advantages of enzyme- and nanomaterial-free for signal amplification, as well as homogeneous detection, the developed approach thus holds great potential for the construction of various aptasensors for convenient and sensitive detection of different molecules.

Introduction

Proteins play important roles in all life activities. Particularly, many protein biomarkers can act as indicators of disease nascent stages or pathological conditions. For example, the protein biomarker, platelet-derived growth factor BB (PDGF-BB), one of the critical growth factors, has proved to be related to tumor transformation, growth and progression.[1,2] Therefore, it is of great significance for the identification and quantification of the disease-related proteins in proteomics research, biomedical research and clinical diagnosis.[3] However, most routine methods for the detection of proteins are dependent upon antigen-antibody immunological assays, which encounter several limitations, such as cumbersome operation processes, high cost and low sensitivity.[4-6] Hence, molecular probes based on aptamer-target recognitions have been increasingly used as promising alternative methods over the conventional antibody-based approaches, due to the excellent versatility of nucleic acid probes in labeling, modification, signaling, and amplification.[7]

Aptamers are artificial short oligonucleotides selected from a process of in vitro evolution named systematic evolution of ligands by exponential enrichment (SELEX).[8] Aptamers have specific recognition capabilities toward many molecular targets, including small molecules,[9] proteins[10] and whole cells[11] with high binding affinities. Besides their excellent binding capabilities, aptamers also exhibit other intrinsic superiorities, such as simple synthesis, easy labeling, high stability over traditional antibodies, making them desirable alternative candidates to traditional antibodies for bio-detection applications. Therefore, aptamers as new molecular tools have received tremendous attention in scientific research. To improve the detection sensitivity and selectivity, several amplification means for highly sensitive detection of protein biomarkers have been reported in the past decades.[12,13] Polymerase chain reaction (PCR),[14] rolling circle amplification (RCA)[15] and enzyme-assisted[16] process have been successfully coupled with electrochemical[17] or fluorescent[18] signal transduction approaches to achieve this purpose. For example, the Yu group demonstrated a circular aptameric recognition system based on target binding-triggered RCA.[19] The RCA-based sensing system could take place with the help of polymerase and dNTPs, and the target protein could be displaced by the polymerase. During the polymerization process, numerous short oligonucleotides could be yielded to act as primers for the padlock probes to realize RCA. In this way, extraordinary high sensitivity can be achieved. Although these amplified approaches can achieve high sensitivity, they commonly encounter several limitations, such as high cost and sophisticated assay protocols and instrumentations, for their wide applications. Thus, it is still of high demand and importance to design convenient amplification methods for aptamer-based sensing systems.

In this regard, a new enzyme-free detection strategy based on target-induced function of an aptamer machine is designed herein for sensitive and selective detection of PDGF-BB via strand displacement reactions. The toehold-mediated strand displacement reaction (TSDR), first pioneered by Yurke et al[20] for the construction of dynamic DNA tweezers in the field of DNA nanotechnology, has been explored as a powerful method to control DNA

[a] Key Laboratory of Luminescent and Real-Time Analytical Chemistry, Ministry of Education, School of Chemistry and Chemical Engineering, Southwest University, Chongqing 400715, PR China. Email: yunatswu@swu.edu.cn (Y. Xiang); Tel.: +86-23-68252277.

hybridizations.[21,22] The TSDR is typically triggered by the hybridizations between the fuel strands and the complementary, unpaired toeholds of the duplexes through a process similar to branch migration.[23] The TSDR is effective, specific and can take place spontaneously at room temperature without the involvement of any enzymes, and the kinetic rate can be tuned easily by modulating the strength of the binding toeholds. With these prominent advantages, it provides a useful enzyme-free signal amplification platform for sensitive detection of DNA,[24] RNA,[25] proteins[10] or small molecules.[9] In our protein biomarker sensing design, the target PDGF-BB binds and unfolds the stem-loop structure of the aptamer hairpin probes into the closely packed tight structure, exposing the toeholds originally caged in the hairpin structure. The exposed toeholds further hybridize with the invading DNA duplexes to trigger the TSDR process to initiate the aptamer machine for recycling PDGF-BB autonomously to achieve amplified detection of PDGF-BB.

Experimental

Chemicals and Materials

PDGF-BB was obtained from ExCell Biology Inc. (Shanghai, China). α-Fetoprotein (AFP) was purchased from Abcam Co., Ltd (Shanghai, China). Mouse immunoglobin G (IgG) and thrombin were supplied by Sigma-Aldrich (St, Louis, MO). [Tris(hydroxymethy-l)aminomethane] hydrochloride (Tris-HCl), the hairpin PDGF-BB binding aptamer (H1) and the oligonucleotides (Control H1, DNA1 and DNA2) with the sequences listed as follows were all purchased from Shanghai Sangon Biological Engineering Technology and Services Co., Ltd. (Shanghai, China). H1: 5′-FAM-CGTTCACAGGCACAGGCTACGGCACGTAGAGCATCACCATGATCCTGTGAACG-Dabcyl-3′; Control H1: CGTTCACAGGCACAGGCTACGGCACG*A**T*GAGCA*AG*ACCATGATCCTGTGAACG; DNA1: 5′-CGTT**CACAGGATCATG**-3′; DNA2: 5′-**CATGATCCTGTG**CCTGTGAA-3′ (Note: The italic nucleotides indicated the variation of control H1 to H1; the underlined sequence was the anti-PDGF-BB aptamer and the bold segments showed the binding regions between DNA1 and DNA2Human serums were ordered from Sigma-Aldrich (St. Louis, MO) and stored at -20 °C before use. Other chemical reagents were obtained from Sinopharm Chemical Reagents, Co., Ltd. (Shanghai, China). The chemical reagents (analytical grade) involved in the tests were used as provided. Ultrapure water with specific resistance of 18.25 MΩ•cm was used during the whole experimental processes.

Amplified fluorescent assay of PDGF-BB

Prior to experiments, the PDGF-BB binding aptamer (H1) was heated to 90 °C for 5 min, followed by slowly cooling down to 25 °C in a period of 2 h to obtain the stable hairpin loop-stem structure, and DNA1 and DNA2 were annealed to form the partial duplex fuel probe (PDF) by using the same protocol. Next, various concentrations of PDGF-BB were incubated with the mixture of H1 (200 nM), PDF (200 nM) in 50 μL of Tris-HCl buffer (10 mM Tris-HCl, 140 mM NaCl, 10 mM KCl, 1 mM $MgCl_2$, pH 7.4) for 60 min in the dark at room temperature. Then, the solution was diluted with Tris-HCl buffer to a final volume of 200 μL, and fluorescence intensity measurements were performed to obtain the data.

Native polyacrylamide gel electrophoresis (PAGE) experiment

Native PAGE of different solutions was performed by using a 16% native polyacrylamide gel. Electrophoresis was performed in 1×TBE buffer at 100 V for 90 min. After staining with ethidium bromide, the gel was photographed with a digital camera under ultraviolet light.

Fluorescence measurements

Fluorescent signals of the solutions were recorded by a Shimadzu (Tokyo, Japan) RF-5301-PC fluorescence spectrophotometer using a 150 W Xenon lamp (Ushio Inc., Japan) as the excitation source. The data were collected from 450 to 650 nm by setting the excitation wavelength of 490 nm. The emission and excitation slit widths were respectively set at 5 nm at room temperature.

Results and discussion

Design principle for amplified fluorescent detection of PDGF-BB

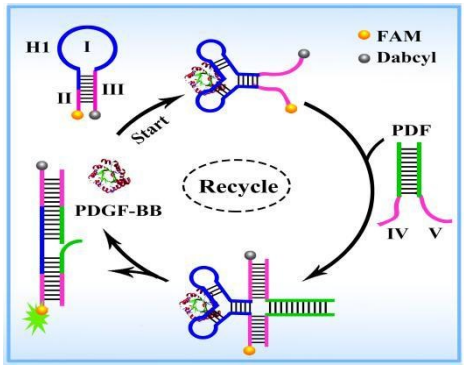

Scheme 1 Schematic principle of the autonomous aptamer machine biosensor for enzyme-free and amplified detection of PDGF-BB.

Our amplified protein detection principle is illustrated in Scheme 1. The system involves two rationally designed DNA probes, the aptamer hairpin (H1) and the PDF strands. The original aptamer sequence of PDGF-BB is designed to be located in the loop and part of stem of H1 (region I), and the toehold regions of II and III are added to the 5′- and 3′-ends of H1 to promote the formation of a stable stem-loop structure and to block them for binding with PDF in the absence of PDGF-BB. A fluorescent dye (FAM)/quencher (Dabcyl) pair is labeled at the two ends of H1, respectively, for signal production. Due to sufficient quenching caused by the close proximity of the fluorophore to the quencher, minimized fluorescence emission is expected with the absence of the target protein. The PDF probe is pre-hybridized with 12 complementary base pairs and the melting temperature (T_m) is estimated to be 46.4 °C (verified by the OligoAnalyzer 3.1 online software fromm Integrated DNA Technologies). Thus, the PDF probe is stable at room temperature, and region IV and V are exposed and reactive to the toeholds for hybridization. Upon the addition of PDGF-BB, the specific binding between the aptamer sequence (region I) and PDGF-BB causes a conformational change of the intramolecular DNA hybridization of H1, and makes it fold into a close-packed tight structure to free the originally caged toehold region II and III to initiate the hybridization with the PDF probe through TSDR. In this case, the target-aptamer complex and the PDF probe first form a

four-stranded complex intermediate, known as a holliday junction. The intermediate holliday junction structure is unstable and a process similar to DNA branch migration along the duplex region occurs, leading to the displacement of PDGF-BB and the separation of the fluorophore and quencher, thereby recovering the fluorescent signals. The released target PDGF-BB can associate with another intact H1 to initiate a new hybridization and strand displacement reaction. Through this autonomous cyclic process, each target protein can induce the unfolding of many H1 to obtain significantly amplified fluorescent signals. Therefore, quantitative detection of PDGF-BB with high sensitivity can be expected by recording the change of fluorescent signals.

Feasibility demonstration of the method

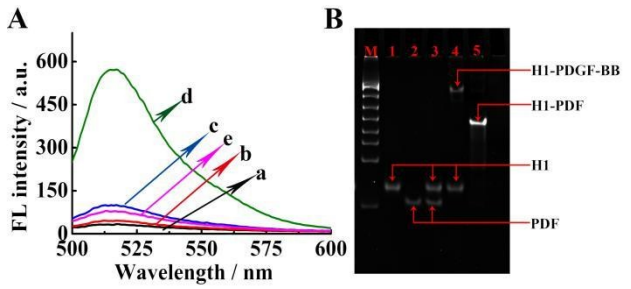

Fig. 1. (A) The fluorescence emission spectra of different solutions incubated at 25 °C for 60 min: (a) H1; (b) H1 and PDF; (c) H1 and PDGF-BB; (d) H1, PDF and PDGF-BB; (e) control H1, PDF and PDGF-BB.The concentrations of H1, PDF and PDGF-BB were 200 nM, 200 nM, and 50 nM, respectively. (B) Native PAGE characterization of the PDGF-BB sensing strategy. Lane M: DNA marker; Lane 1: H1; Lane 2: PDF; Lane 3: H1 and PDF; Lane 4: H1 and PDGF-BB; Lane 5: mixture of H1, PDF and PDGF-BB. The concentrations of H1, PDF and PDGF-BB were 500 nM, 500 nM, and 100 nM, respectively.

To test the feasibility of our designed system, the fluorescence emissions of different solutions were recorded. As shown in Fig. 1A, the solution of H1 shows a low fluorescence intensity (curve a) at 520 nm because of the high quenching efficiency of Dabcyl to FAM. When the PDF probe is incubated with H1, the solution exhibits a negligible change in fluorescence intensity (curve b) because the toehold regions are blocked in the stem of H1 and therefore the TSDR reaction is inhibited. While, the introduction of PDGF-BB (50 nM) to H1 leads to an apparent increase in fluorescence intensity (curve c), demonstrating the association of PDGF-BB with the aptamer sequence to cause conformational change of H1 and the separation of the fluorophore/quencher pair. In addition, upon the addition of the target PDGF-BB (50 nM) to the mixture of H1 and PDF, a significant enhancement of fluorescence intensity (curve d) against the addition of the PDF probe or the target protein to H1 is observed. Moreover, the incubation of PDGF-BB with the mixture of a control H1 (with four nucleotides variation to H1) and PDF shows similar fluorescence intensity (curve e) to that of the mixture of H1 and PDF without the presence of PDGF-BB (curve b), indicating that control H1 is unable to bind PDGF-BB after sequence modification. These comparisons indicate the remarkable signal amplification capability of the target responsive autonomous aptamer machine. Native PAGE experiment was also performed to verify our PDGF-BB sensing mechanism. As illustrated in Fig. 1B, the mixture of H1 and PDF (Lane 3) shows two distinct bands corresponding to H1 (Lane 1) and PDF (Lane 2), respectively, demonstrating the co-existence of H1 and PDF in the absence of PDGF-BB. While, the mixture of H1 and PDGF-BB generates a new band with much lower electrophoretic mobility (Lane 4), due to the successful binding of PDGF-BB to H1. Moreover, the incubation of PDGF-BB with H1 and PDF leads to the appearance of the band of the H1-PDF complex (Lane 5), suggesting the proposed TSDR reaction. These results are in agreement with the demonstrations in Fig. 1A, verifying the feasibility our method.

Experimental optimizations

To obtain the desirable analytical performance of the sensing system, the concentration of the PDF probe and reaction time were respectively optimized. The concentration of the PDF probe has a significant impact on the specificity and efficiency of the system. On the one hand, a higher concentration of the PDF probe may result in higher background fluorescent noise due to the non-specifically induced hybridizations. On the other hand, low concentration of the PDF probe may have a negative effect on the efficiency of the TSDR reaction. Therefore, we first investigated the effect of the concentration of the PDF probe with H1 fixed at 200 nM. As depicted in Fig. 2A, when 50 nM PDGF-BB is introduced into the system (with 60 min reaction time), increasing concentration of the PDF probe from 100 to 400 nM leads to gradual increase of the fluorescent signal (violet bars in Fig. 2A). Meanwhile, the background noise (F_0) also gradually increases (green bars in Fig. 2A) in the absence of the target protein, which is possibly caused by the partial self-hybridization between H1 and the PDF probes. The synergistic effect thus leads to a maximum signal-to-background ratio (F/F_0) at the concentration of 200 nM. Thus, 200 nM of the PDF probe is selected as the optimal concentration in the following experiments. The incubation time is another key factor that can directly influence the efficiency of equilibrium reaction between PDGF-BB and H1 and subsequent strand displacement reaction rate. Therefore, in order to achieve optimal assay conditions, the reaction time was optimized. As displayed in Fig. 2B, when PDGF-BB is added, the fluorescent signal increases sharply from 20 min to 60 min and then reaches a plateau thereafter (violet bars in Fig. 2B). At the meantime, for the blank, the fluorescence intensity also increases gradually (green bars in Fig. 2B), and the maximum value of F/F_0 is obtained at 60 min, which is selected as the optimal reaction time in the following experiments.

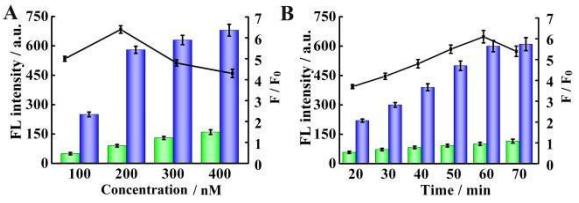

Fig. 2. Effects of (A) the concentration of the PDF probe (with 60 min incubation time) and (B) incubation time (with the PDF probe fixed at 200 nM) on the value of F/F_0 (F and F_0 corresponded to the presence and absence of 50 nM PDGF-BB, respectively). Error bars, SD, n = 3.

Analytical performance of the sensing method

After optimizing the experimental parameters, the changes of fluorescence emission intensity with different concentrations of PDGF-BB were recorded to demonstrate the sensitivity of the current assay. As shown in Fig. 3A, it is clear that the fluorescence intensity increases accordingly with elevated concentration of PDGF-BB from 0 pM to 100 nM (curves a to h). Meanwhile, in Fig. 3B, a proportional relationship in the range of 10 pM to 100 nM is obtained with a linear regression equation of y = 125.35 x + 363.55 (R^2 = 0.9976, y and x represent the fluorescent signal and the logarithmic value of the concentration of PDGF-BB, respectively), and the detection limit of the assay is determined to be 3.2 pM based on the 3 σ rule. Such a high sensitivity of the aptasensor significantly exceeds other conventional fluorescent approaches without the involvement of any signal enhancement means[26,27] and is comparable to those with complicated enzyme-assisted or nanomaterial-based amplification assays for PDGF-BB.[28,29] In addition, according to six repetitive measurements for the detection of 10 nM PDGF-BB, a relative standard deviation of 5.3% is obtained, indicating desirable reproducibility of the sensor for protein assay.

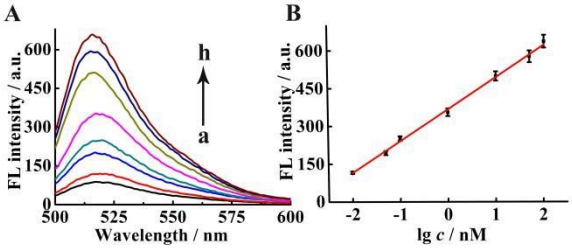

Fig. 3. (A) Fluorescence responses of the proposed strategy to various concentrations of PDGF-BB. From a to h: (a) 0 pM, (b) 10 pM, (c) 50 pM, (d) 100 pM, (e) 1 nM, (f) 10 nM, (g) 50 nM, (h) 100 nM. (B) The resulting calibration curve for fluorescence intensity vs. the logarithmic concentration of PDGF-BB (from 10 pM to 100 nM). Error bars, SD, n = 3.

Selectivity also has a crucial effect on the evaluation of the fabricated aptasensor. Especially, for the aptamer-based system, modulating the length and sequence of the aptamer may pose a great influence (deterioration or improvement) on its recognition and binding ability,[30] which may affect the selectivity of the aptasensor. Thus, experiments were carried out to verify the selectivity of the detection method by using other control proteins, including AFP, mouse IgG and thrombin, under optimized conditions. According to the results shown in Fig. 4, The addition of 10-fold excess of the control proteins (each at the concentration of 500 nM) to the sensing solution causes insignificant fluorescence intensity change compared with the blank test (without target protein). In contrast, the introduction of a lower concentration of the target PDGF-BB (50 nM) leads to a substantial increase of fluorescence intensity. Such an obvious comparison indicates the inherent high specific binding capability of the aptamer sequence to the target protein. In other words, only the presence of PDGF-BB can lead to the conformation change of the stem-loop hairpin structure to initiate subsequent amplification cycles.

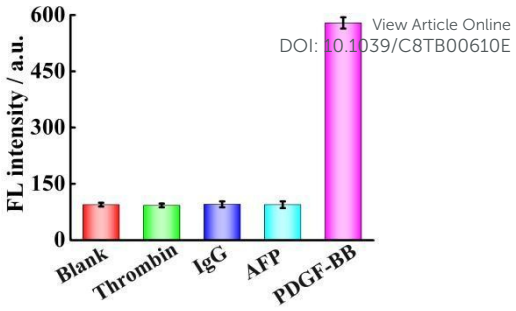

Fig. 4. Selectivity of the sensing method for the target PDGF-BB against other control proteins (AFP, Thrombin and IgG). The concentration of PDGF-BB was 50 nM and all other proteins were 500 nM. Error bars, SD, n = 3.

Table 1 Determination of PDGF-BB in serum samples (n=6).

Samples	Added (pM)	Found (pM) (mean ± RSD)	Recovery (%)
1	10	10.2 ± 1.4	102
2	50	48.1 ± 2.9	96.2
3	100	103.6 ± 3.4	103.6

Detection of PDGF-BB in real samples

For real application of the sensing strategy, the developed detection method should be able to apply for complex biological samples. Thus, to evaluate the feasibility and potential applicability of the system, various concentrations of PDGF-BB were spiked into 10-fold diluted human serum samples (with Tris-HCl buffer) and recovery tests were carried out. The results were listed in Table 1. It can be seen that the recovery rates for the spiked PDGF-BB fall within the range from 96.2 to 103.6% with the relative standard deviations below 3.4%, indicating the developed sensor functions well in complex real samples and holds great potential for further applications.

Conclusions

To conclude, a simple enzyme-free signal amplification strategy has been constructed for highly sensitive detection of PDGF-BB based on the combination of the target binding-induced conformational change of aptamers and TSDR. The association of PDGF-BB with the aptamer leads to conformational switching of the aptamer hairpin probes and further triggers the TSDR to recycle the target proteins to generate significantly amplified fluorescent signals. Due to the high affinity and specific recognition between the probes and proteins, the method shows high selectivity and sensitivity with a detection limit down to 3.2 pM for PDGF-BB. Besides, our approach avoids the addition of enzymes or nanomaterials for signal amplification, eliminating the troublesome washing and separation steps or complicated synthesis processes required in common signal amplification assays. The method demonstrated herein can thus be extended as a universal strategy for detecting various protein or small molecules at low levels.

Conflicts of interest

There are no conflicts to declare.

Acknowledgements

This work was supported by National Natural Science Foundation of China (No. 21675128) and Fundamental Research Funds for the Central Universities (XDJK2017A001).

Notes and references

1 S. Minardi, L. Pandolfi, F. Taraballi, X. Wang, E.D. Rosa, Z.D. Mills, X.W. Liu, M. Ferrari and E. Tasciotti, *ACS Appl. Mater. Interfaces.*, 2017, **9**, 14566.
2 J. Zheng, M. Zhang, X.H. Guo, J.P. Wang and J.L. Xu, *Sens. Actuators B*, 2017, **250**, 8.
3 B.J. Jeong, R. Akter, O.H. Han, C.K. Rhee and M.A. Rahman, *Anal. Chem.*, 2013, **85**, 1784.
4 Y.N. Tang, Z.X. Wang, X.L. Yang, J.B. Chen, L.N. Liu, W.A. Zhao, X.C. Le and F. Li, *Chem. Sci.*, 2015, **6**, 5729.
5 X.D. Deng, M.S. Chen, Q. Fu, N.M.B. Smeets, F. Xu, Z.Y. Zhang, C.D.M. Filipe and T. Hoare, *ACS Appl. Mater. Interfaces.*, 2016, **8**, 1893.
6 Z.H. Yang, Y. Zhuo, R. Yuan and Y.Q. Chai, *Anal. Chem.*, 2016, **88**, 5189.
7 B.Y. Jiang, F.Z. Li, C.Y. Yang, J.Q. Xie, Y. Xiang and R. Yuan, *Anal. Chem.*, 2015, **87**, 3094.
8 H.G. Sun and Y.L. Zu, *Small*, 2015, **11**, 2352.
9 J.H. Park, J.Y. Byun, W.B. Shim, S.U. Kim and M.G. Kim, *Biosens. Bioelectron.*, 2015, **73**, 26.
10 Z.A.I. Mazrad, K. Lee, A. Chae, I. In, H. Lee and S.Y. Park, *J. Mater. Chem. B*, 2018, **6**, 1149.
11 Z. Fan, L.M. Sun, Y.J. Huang, Y.Z. Wang and M.J. Zhang, *Nature* Nanotech., 2016, **11**, 388.
12 H. Wu, K. Zhang, Y.L. Liu, H.Y. Wang, J. Wu, F.F. Zhu and P. Zou, *Biosens. Bioelectron.*, 2015, **64**, 572.
13 H.Q. Zhang, M.D. Lai, A. Zuehlke, H.Y. Peng, X.F. Li and X.C. Le, *Angew. Chem. Int. Ed.*, 2015, **54**, 14326.
14 P.V. Robinson, C.T. Tsai, A.E. De Groot, J.L. Mckechnie and C.R. Bertozzi, *J. Am. Chem. Soc.*, 2016, **138**, 10722.
15 Y. Zhu, H.J. Wang, L. Wang, J. Zhu and W. Jiang, *ACS Appl. Mater. Interfaces.*, 2016, **8**, 2573.
16 D.Q. Fan, C.T. Wu, K. Wang, X.X. Gu, Y.Q. Liu and E.K. Wang, *Chem. Commun.*, 2016, **52**, 406.
17 P.H. Ling, Q. Hao, J.P. Lei and H.X. Ju, *J. Mater. Chem. B*, 2015, **3**, 1335.
18 Z. Zhang, C. Hejesen, M.B. Kjelstrup, V. Birkedal and K.V. Gothelf, *J. Am. Chem. Soc.*, 2014, **136**, 11115.
19 Z.S. Wu, H. Zhou, S.B. Zhang, G.L. Shen and R.Q. Yu, *Anal. Chem.*, 2010, **82**, 2282.
20 B. Yurke, A.J. Turberfield, A.P. Mills Jr, F.C. Simmel and J.L. Neumann, *Nature*, 2000, **406**, 605.
21 P. Šulc, T.E. Ouldridge, F. Romano, J.P. Doye and A.A Louis, *Biophys. J.*, 2015, **108**, 1238.
22 F.A. Wang, J. Elbaz and I. Willner, *J. Am. Chem. Soc.*, 2012, **134**, 5504.
23 N. Srinivas, T.E. Ouldridge, P. Šulc, J.M. Schaeffer, B. Yurke, A.A. Louis, J.P. Doye and E. Winfree, *Nucleic Acids Res.*, 2013, **41**, 10641.
24 D.A. Khodakov, A.S. Khodakova, D.M. Huang, A. Linacre and A.V. Ellis, *Sci. Rep.*, 2015, **5**, 8721.
25 X. Li, D.X. Li, W.J. Zhou, Y.Q. Chai, R. Yuan, and Y. Xiang, *Chem. Commun.*, 2015, **51**, 11084.
26 S. Ranallo, M. Rossetti, K.W. Plaxco, A. Vallée-Bélisle and F. Ricci, *Angew. Chem. Int. Ed.*, 2015, **54**, 13214.
27 D.S. Zhu, J. Zhu, Y. Zhu, L. Wang and W. Jiang, *Chem. Commun.*, 2014, **50**,14987.
View Article Online
DOI: 10.1039/C8TB00610E
28 L.P. Qiu, Z.S. Wu, G.L. Shen, R.Q. Yu, *Anal. Chem.*, 2011, **83**, 3059.
29 S.J. Ye, X.M. Zhai, Y.Y. Wu, S.P. Kuang, *Biosens. Bioelectron.*, 2016, **79**, 130.
30 D. Musumeci and D. Montesarchio, *Pharmacol Ther.*, 2012, **136**, 202.

View Article Online
DOI: 10.1039/C8TB00610E

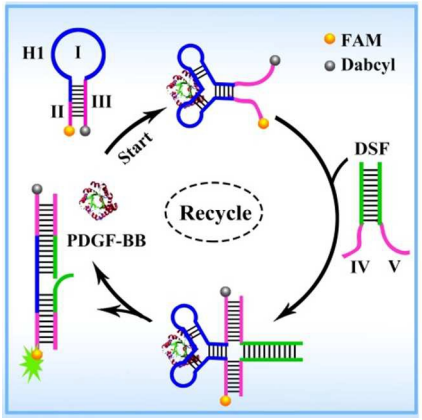

Target-triggered operation of the aptamer machine leads to amplified and highly sensitive detection of protein biomarkers.